
This copy is for your personal, non-commercial use only.

If you wish to distribute this article to others, you can order high-quality copies for your colleagues, clients, or customers by [clicking here](#).

Permission to republish or repurpose articles or portions of articles can be obtained by following the guidelines [here](#).

The following resources related to this article are available online at www.sciencemag.org (this information is current as of September 25, 2014):

Updated information and services, including high-resolution figures, can be found in the online version of this article at:

<http://www.sciencemag.org/content/315/5816/1235.full.html>

A list of selected additional articles on the Science Web sites **related to this article** can be found at:

<http://www.sciencemag.org/content/315/5816/1235.full.html#related>

This article has been **cited by** 1 articles hosted by HighWire Press; see:

<http://www.sciencemag.org/content/315/5816/1235.full.html#related-urls>

This article appears in the following **subject collections**:

Atmospheric Science

<http://www.sciencemag.org/cgi/collection/atmos>

Hurricane Intensity and Eyewall Replacement

Robert A. Houze Jr.,^{1*} Shuyi S. Chen,² Bradley F. Smull,¹ Wen-Chau Lee,³ Michael M. Bell³

Observations made during the historic 2005 hurricane season document a case of “eyewall replacement.” Clouds outside the hurricane eyewall coalesce to form a new eyewall at a greater radius from the storm center, and the old eyewall dies. The winds in the new eyewall are initially weaker than those in the original eyewall, but as the new eyewall contracts, the storm reintensifies. Understanding this replacement mechanism is vital to forecasting variations in hurricane intensity. Processes in the “moat” region between the new and old eyewall have been particularly unclear. Aircraft data now show that the moat becomes dynamically similar to the eye and thus is converted into a region inimical to survival of the inner eyewall. We suggest that targeting aircraft to key parts of the storm to gain crucial input to high-resolution numerical models can lead to improvements in forecasting hurricane intensity.

The tragedy of Hurricane Katrina in 2005 redoubled attention to the problem of tropical cyclone forecasting. Although forecasts of hurricane tracks and landfall location have improved in recent decades, forecasting of hurricane intensity (how strong the wind will be at landfall) has not (1). This comparative state of progress is not surprising, because a storm’s track is primarily determined by the large-scale environment in which the tropical cyclone is embedded. Improvements in models that forecast surrounding large-scale wind patterns, combined with extra aircraft and satellite observations in the environments of storms, have thus led to improved track forecasts.

Changes of intensity (as measured by maximum surface wind strength) are more challenging to anticipate. Rapid changes of storm intensity are connected with the detailed spatial arrangement and unsteady pattern of smaller-scale cloud and precipitation features internal to the storm. These features are not resolved by large-scale models and are particularly difficult to observe because data must be obtained in the active central portion of the storm, where internal structural changes are taking place, while the storm is still over the ocean.

Eyewall replacement—a key process in hurricane intensity change. In a tropical cyclone, the radius of maximum wind is located in a circular region of heavily precipitating cloud called the “eyewall,” which encircles the relatively calm “eye” of the storm. Outside the eyewall are lines of convective cloud that spiral in toward the eyewall and are called “rainbands.”

In the 1960s and 1970s, R. H. Simpson and J. S. Malkus hypothesized that cloud seeding could reduce hurricane intensity (2). The strategy was to use aircraft to seed rainbands located outside the original eyewall in such a way as to form a circular ring of deep clouds around the storm that would take over as a new eyewall and choke off the old eyewall. Once the inner eyewall weakened, the outer eyewall would contain the strongest winds in the storm, but because the new eyewall formed farther from the storm center, these winds would be weaker than in the original eyewall. If this change of storm intensity could be induced just before landfall, a storm moving ashore would produce less damage.

The cloud-seeding approach ultimately proved ineffective (3, 4). Many strong, mature tropical cyclones exhibit a natural “eyewall replacement” process (5) in which a new (outer) eyewall takes over from the original (inner) eyewall, just as had been hypothesized—but with no cloud seeding taking place. Theoretical studies further show that the new eyewall’s dynamics may cause it to contract over time (6). After an outer eyewall forms and envelops the inner eyewall, and the storm deintensifies, the new larger-diameter eyewall itself may shrink in radius, so that the storm reintensifies. This process may repeat itself. As additional new eyewalls form, the storm may undergo one or more large oscillations in intensity by natural processes alone. Therefore, the focus has changed: Instead of producing such changes artificially, by seeding, the goal is to forecast the intensity changes occurring as a result of natural eyewall replacement.

A field experiment revealing the process of eyewall replacement. The difficulty in forecasting when eyewall replacement will and will not occur was a key factor motivating the Hurricane Rainband and Intensity Change Experiment (RAINEX) in 2005 (7), in which an innovative set of aircraft measurements

were obtained in Hurricanes Katrina, Ophelia, and Rita. The premise was that the variations in intensity occurring in conjunction with eyewall replacement involve interactions of the rainbands with each other, with the eyewall, and with the large-scale environment. The aircraft therefore focused on documenting detailed aspects of the specific rainbands and eyewalls that appear most likely to interact and affect intensity changes.

In carrying out this mission, RAINEX did three things differently from past hurricane observational efforts (7). First, RAINEX deployed the Naval Research Laboratory’s (NRL) P-3 aircraft equipped with the National Center for Atmospheric Research (NCAR) ELDORA (Electra Doppler radar) (8), the highest quality meteorological airborne Doppler available, never before used in hurricanes. This research platform was flown in coordination with two Doppler-radar-equipped P-3 aircraft operated by the National Oceanic and Atmospheric Administration (NOAA) (9). Second, satellite communications and specialized interactive visualization technology were used to transmit, accumulate, and combine the data from aircraft radars, coastal radars, and satellite data onto a continuously updated master chart in the operations center with all the aircraft positions and tracks. This integrated map, which provided a wider and more comprehensive view of the detailed storm structure and situation than is possible from a single aircraft’s radar, made it possible for a ground controller to optimally coordinate the flights of the three P-3 aircraft to observe those small-scale features most likely associated with intensity changes. Third, high-resolution (1.67 km) model forecasts of the investigated storms were made in real time to aid flight planning. These forecasts used input from larger-scale models (7). In the future, high-resolution forecasts of tropical cyclone intensity can potentially make use of the sort of detailed real-time ground-controlled aircraft observations obtained in RAINEX. Ground control can systematically target the measurements to small-scale features deemed most likely to affect intensity changes and assimilate these key observations back into the models.

Figure 1 shows a sequence of the high-resolution model forecasts of the structure of Hurricane Rita made during RAINEX. They show three stages of the storm’s development, during a period when eyewall replacement occurred over the Gulf of Mexico. Comparison with radar data shows that the simulated structures and sequence of events were very similar to those captured by airborne observations of the actual storm. Figure 1A shows a closed annulus of heavy rain in the center of the panel. This was the original eyewall. To its west and east were spiral rainbands, intense cores of heavy rain aligned in curved bands angling in toward and becoming tangent to the eyewall. Figure 1B

¹Department of Atmospheric Sciences, University of Washington, Seattle, WA 98195–1640, USA. ²Rosenstiel School of Marine and Atmospheric Sciences, University of Miami, Miami, FL 33149, USA. ³Earth Observing Laboratory, National Center for Atmospheric Research, Boulder, CO 80307, USA.

*To whom correspondence should be addressed. E-mail: houze@atmos.washington.edu

shows that 28 hours later, eyewall replacement had begun. The rainbands had organized into a coherent circular feature. A more weakly precipitating annular zone, which we call the moat, separated this new outer eyewall from the inner eyewall, which itself had begun to weaken. The process by which the second eyewall forms, although it happens frequently in nature, is not fully understood. One school of thought is that circular flow pattern around the center of the storm spawns small-scale disturbances called “vortex Rossby waves,” which propagate radially outward from the original eyewall region (10). Depending on the exact structure of the hurricane vortex, the waves may act to concentrate angular momentum at a critical radius where their phase velocity matches the mean swirling flow and in this way coalesce to form a new outer eyewall. Another idea is that the large-scale humidity field surrounding the storm can affect the structure of the rainbands at a certain radius, which may lead to a second eyewall formation (11). Figure 1C shows that the inner eyewall had nearly vanished, while the outer eyewall, which was replacing it, was taking shape at a somewhat greater radius. The maximum winds in the storm had decreased from about 70 m s^{-1} to 52 m s^{-1} . Also notable is that the new eyewall had a smaller radius in Fig. 1C than in Fig. 1B, indicating that it had begun to contract, as expected from theory (6).

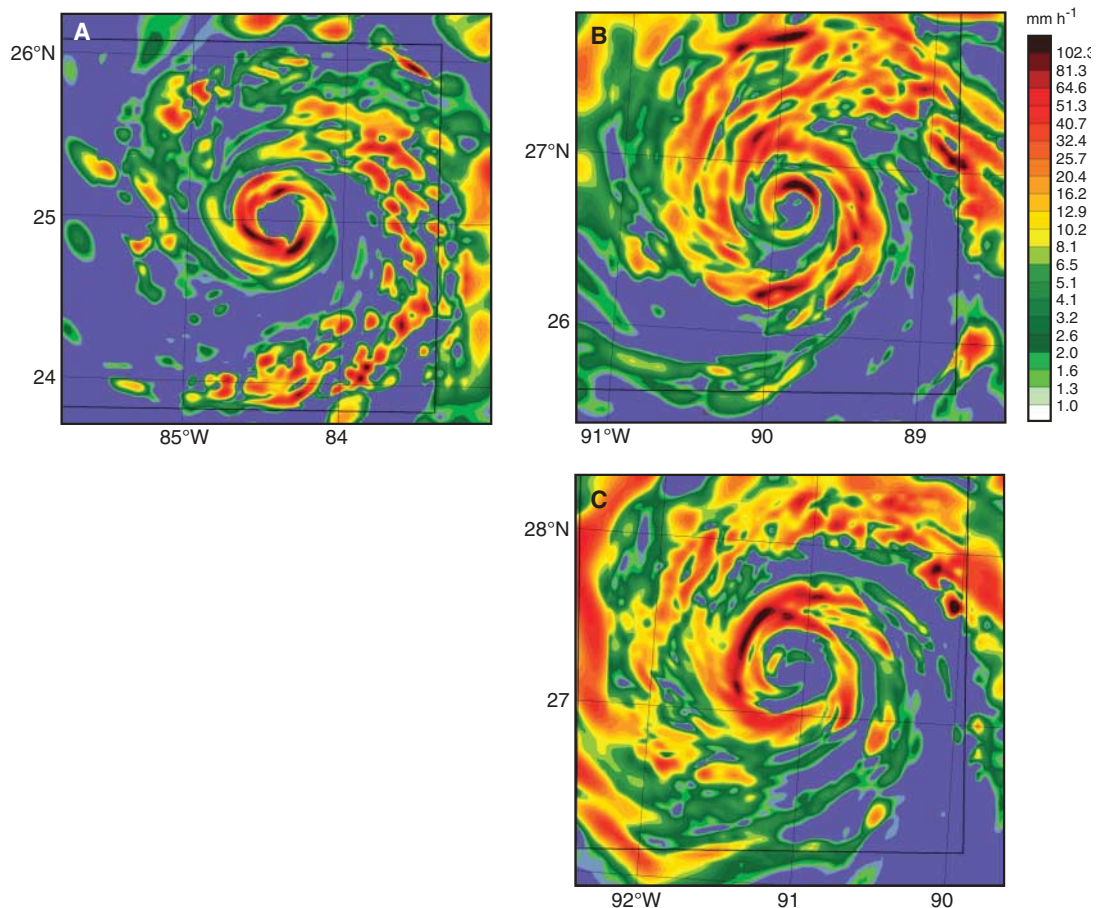
Aircraft radar data collected in Rita (Fig. 2) confirmed the double eyewall structure suggested by the model forecast. The NRL P-3 with ELDORA concentrated on the inner portion of the storm by flying in a circular fashion, repeatedly circumnavigating the inner core of the storm (Fig. 2A). Figure 2B shows the radar echo detected by ELDORA. Because the radar receives microwave radiation backscattered from precipitation particles in the path of the beam (12), the echo intensity pattern (color shading in Fig. 2B) indicates the precipitation pattern. The data clearly show two concentric eyewalls with a circular moat of weak echo between them. This pattern compares favorably to the simulated precipitation pattern (Fig. 1B), although the model timing was ~ 6 to 7 hours too fast.

The inner eyewall (Fig. 2B) was still fairly strong, although its southeast side had weakened, just as it did in the model forecast once the new eyewall surrounded it (Fig. 1B). A distinct wind maximum accompanied each eyewall (7). Because the Doppler radar scanned approximately orthogonal ($\pm 70^\circ$) to the track (8), the circular flight path gave a continuous view of the two eyewalls and their interactions. The cells of heavy precipitation in the outer eyewall seen in Fig. 2B are of a scale of detail not seen in hurricanes before the use of ELDORA in RAINEX. The cells produced by small-scale intense air motions tend to be elongated and distributed in-

termittently around the outer eyewall. Recent theoretical studies (e.g., 10, 13) have shown that as a new eyewall forms, small-scale air motion features generated in rainbands gather into an incipient eyewall. ELDORA indicates that this process was likely taking place in this young secondary eyewall.

The moat takes on the characteristics of a hurricane eye. Figure 2C shows the detailed wind field inferred by established methods (14, 15) from ELDORA’s measurement of precipitation particle motions (12). This cross section is a snapshot of the profound new information gained in this study. The moat region between the two eyewalls is occupied throughout its volume by downward air motion. An earlier study of aircraft radar data obtained on radial flight legs crossing a storm with two eyewalls had shown some indications of downward motion in the moat (16). However, because the aircraft with the ELDORA in Rita was ground-controlled to fly in a circle between the two eyewalls (Fig. 2A), we were able to show that the downward motion in the moat extended from upper to lower levels and all around the storm. Figure 2D is a composite of all the data collected during the ELDORA circumnavigation of Rita. It shows quantitatively how this pervasive downward motion determined the mean structure of the entire moat. The dynamics of the moat were transitioning to those of an eye.

Fig. 1. Forecast of surface rainfall intensity in Hurricane Rita. (A) 0715 UTC 21 September, (B) 1115 UTC 22 September, (C) 1715 UTC 22 September. Colors show the rainfall rate (mm h^{-1}) at the sea surface generated by the University of Miami’s high-resolution, vortex-following, coupled atmosphere-wave-ocean version of the fifth-generation Pennsylvania State University/NCAR nonhydrostatic mesoscale model (MM5) (34) operating at a horizontal resolution of 1.67 km. Initial fields at 0000 UTC 20 September 2005 and lateral boundary conditions are from the NOGAPS global numerical forecast model (35).



The eye is a region of singular dynamics determined by the spinning motion of the air in the eyewall, the buoyancy of the cloudy air in the eyewall, the large-scale environment of the storm, and the thermodynamic and turbulent character of the ocean surface. In the initial stages of a tropical cyclone, before a closed eyewall forms, convective clouds occur in ambient air, whose condition is characteristic of the

large-scale atmospheric conditions in the region (17). Once formed, a circular eyewall effectively fences off a portion of the environment air. The trapped air is then modified by the near-field effect of the eyewall. Latent heat released in the surrounding eyewall cloud induces a circulation that draws low-level air out of the eye region (18), causing air farther aloft within the eye to subside. Consequently, the air in the eye is very

dry (19) except for the layer of air in contact with the ocean. Temperature and moisture profiles obtained every 30 to 60 km by dropsondes (20) along the NRL aircraft track (Fig. 2A) show the dryness (relative humidity generally well below 100%) above 1000 m in the eye of Rita (Fig. 3A, green and red curves). Similar dryness seen above 1000 m in the moat (Fig. 3A, blue curve) together with the downward motion throughout the zone between the old and new eyewall (Fig. 2, C and D) suggests that the moat region was not a passive void between the two eyewalls. It was a dynamic entity that would take on the characteristics of an eye and join with the original eye, thus snuffing out the original eyewall.

Conceptual model of a hurricane undergoing eyewall replacement. Figure 4 conceptualizes our view of the eyewall replacement in Rita. The center portion consisting of the eye and the old eyewall reflects a conventional picture of eye dynamics. Immediately outside the original storm core, the new eyewall and moat mimic the old eyewall and eye, respectively. To describe the replacement, we first consider the conventional eye structure in the center of the diagram. The old eyewall circulation draws in near-surface air both from outside the eyewall and from within the eye itself (6). The air in the eye sinks to compensate for this transfer of air into the eyewall (18). Also contributing to the subsidence in the eye is turbulent mixing of angular momentum at the interface of the rapidly rotating eyewall and more quiescent eye region (21). The subsidence warms and dries the air within the eye, thus producing the cloud-free hole commonly characterizing the center of these storms in satellite imagery (Fig. 2A). Near the ocean surface the drying is counteracted by strong turbulent mixing, which transfers water vapor and sea spray from the warm and choppy sea surface upward and maintains high humidity in the lowest layer of the eye. The air at low levels within the inner eye draws energy from the sea more effectively because it is at low pressure (so that the moist enthalpy in equilibrium with the sea is elevated) and because strong winds whipping the moisture off the sea surface often extend well inward from the eyewall. The moisture in the lower layer is also maintained by air near the ocean surface that flows under rather than turning upward into the eyewall, and by a thin layer of moist air cascading down the inner edge of the eyewall. This cascade is produced by cloudy air mixing with the dry air at the inner edge of the eyewall (18). In simplest terms, the eye of the storm thus has a two-layer structure: moist at low levels, with dry descending air above. Capping the moist layer is a stable layer produced by the subsidence. In strong storms, the stable layer capping the lower moist mixed layer takes the form of an "inversion" (temperature increasing with height).

Our conceptual model (Fig. 4) depicts the moat during the replacement as taking on the dynamic behavior of a hurricane eye when

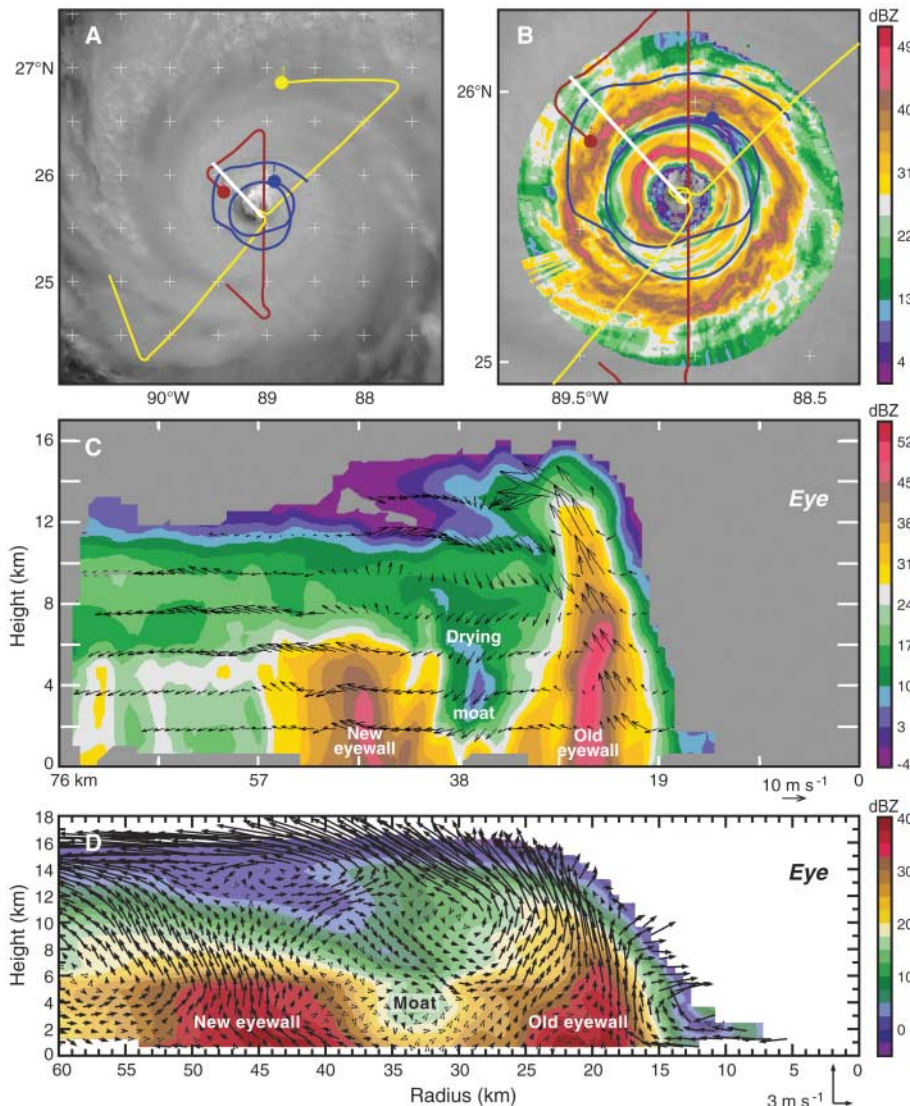


Fig. 2. Aircraft data collected in Hurricane Rita between 1800 and 1820 UTC 22 September 2005. (A) and (B) are plan views; (C) is a vertical cross section across the northwest side of the storm (along the white line in the plan views). Colored lines in (A) denote the flight tracks of the three RAINEX aircraft: yellow and red are the NOAA aircraft tracks; blue is the NRL aircraft, which was instrumented with ELDORA. The dots show aircraft locations as of 1830 UTC. The yellow track segment is for the 80 min preceding that time; the red and blue track segments are for the preceding 45 min. The yellow NOAA track was part of a wide pattern to determine the broad-scale structure of the cyclone vortex. The red NOAA track was part of an intermediate pattern, with shorter legs across the center of the storm to monitor the two eyewalls. The blue NRL track was the circumnavigation that obtained the key radar and sounding data referred to in this article. The color shades in (B) and (C) correspond to values of radar reflectivity (a measure of precipitation intensity). (D) depicts a comprehensive mean of dual-Doppler storm-relative winds derived from ELDORA data obtained during the period 1800 to 1820 UTC while the NRL aircraft that was flying in the moat circumnavigated the storm. Vectors show the component of air motions within the cross-sections [(C) and (D)].

environmental air trapped in the zone between the old and new eyewalls is forced to sink, warming and drying in the process—just as the eye itself formed dynamically when air from the environment was surrounded by and responded to the original eyewall. Dropsondes obtained along the circular flight track in the moat (Fig. 2A) support the idea that the moat was undergoing just such a transition. Depicted dropsonde data was obtained in the eye of Rita at approximately the time the hurricane became the fourth strongest ever observed in the Atlantic basin (Fig. 3, green curves). The eye exhibited high humidity in the first 500 m above the ocean, capped by an extreme temperature inversion (temperature increasing upward to $\sim 27^{\circ}\text{C}$ at 2 km). Dropsondes in the eye on the next day (red curves) showed that as the storm weakened owing to the observed eyewall replacement process, the capping stable layer in the eye became less pronounced (22) and turbulent mixing at low levels was able to extend the moist layer up to about 1200 m. In the moat (blue curves), the humidity and

temperature structure were essentially identical to those in the eye at the time of the replacement. Thus, both the airborne Doppler radar data (Fig. 2, C and D) and dropsondes (Fig. 3) obtained in Rita on 22 September show conditions within the moat taking on the characteristics of an eye.

Once the dynamics of Rita's moat region resembled those of an eye, the inner eyewall could only weaken with time. The bulk of the low-level inflow of high-energy air from the large-scale environment was robbed by the new outer eyewall (note that inflow toward the eye is absent at low levels between the new eyewall and old eyewall in Fig. 2, C and D). The old eyewall was ultimately destroyed by this lack of environmental inflow combined with active downward motion induced by the new eyewall, which evaporated the eyewall clouds and warmed the air surrounding the inner eyewall so that the old eyewall's buoyancy decreased. The progression of the eyewall replacement in Rita observed by radar (Fig. 2) was forecast accurately (Fig. 1). However, when the model resolution was degraded from 1.67 km to about 5 km, simulated eyewall replacement failed

to occur, which indicates that the eyewall replacement dynamics are fundamentally small-scale and require high-resolution modeling to be accurately represented and forecast.

Even though Rita's second eyewall had enclosed the original eyewall by the time of Fig. 2, the inner eyewall remained strong for 12 hours (indicated by tall and intense inner-eyewall radar echoes, as in Fig. 2C). This slow demise of the inner eyewall is typical of hurricanes undergoing eyewall replacement (5). Because the inner eyewall was cut off from the large-scale environment, we conclude that the inner eyewall was drawing some energy from within the storm's inner core. As indicated in Fig. 4, the eyewall draws warm, moist air from the lower portion of the eye into its upward circulation (18). This air provides fuel to the old eyewall. The inner eyewall can apparently survive through this mechanism for several hours before finally expiring. Recent work (23, 24) has suggested that when small-scale vortices form along the inner eyewall (25), the low-level eye air is more efficiently entrained into the eyewall. ELDORA data in Rita document the existence of a well-defined small-scale vortex on the inner edge of the inner eyewall at about the time of Fig. 2. We suspect it contributed to maintaining the intensity of the inner eyewall.

Possible new approaches to forecasting hurricane intensity changes. Eventually, Rita's inner eyewall died and was replaced by the outer eyewall. In conjunction with this eyewall replacement, Rita decreased from category 5 intensity (26, 27) on 21 September, with maximum winds of 77 m s^{-1} , to category 3 or 4 on 22 September 2005, with maximum winds of 50 to 60 m s^{-1} (28). Figure 1 suggests that with a sufficiently high-resolution model, the eyewall replacement and accompanying intensity decrease can be forecast. In addition, the successful documentation of the eyewall replacement process in Rita during RAINEX by ground-controlled aircraft-targeting of the small-scale features internal to the tropical cyclone vortex could be a harbinger of improved forecasting of hurricane intensity. The adoption of real-time targeting of

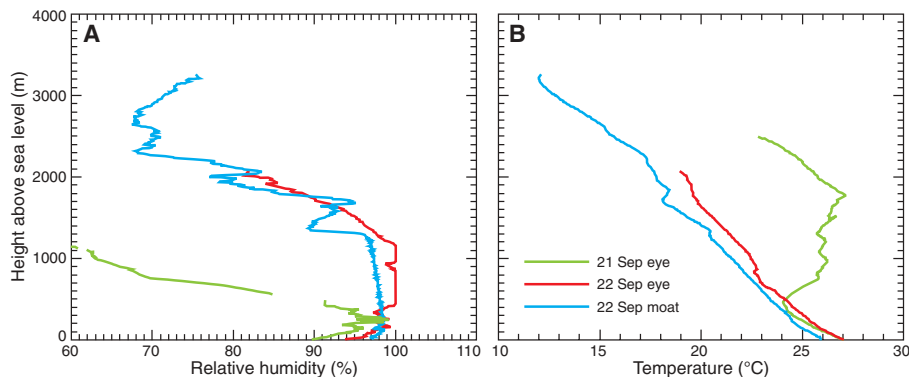
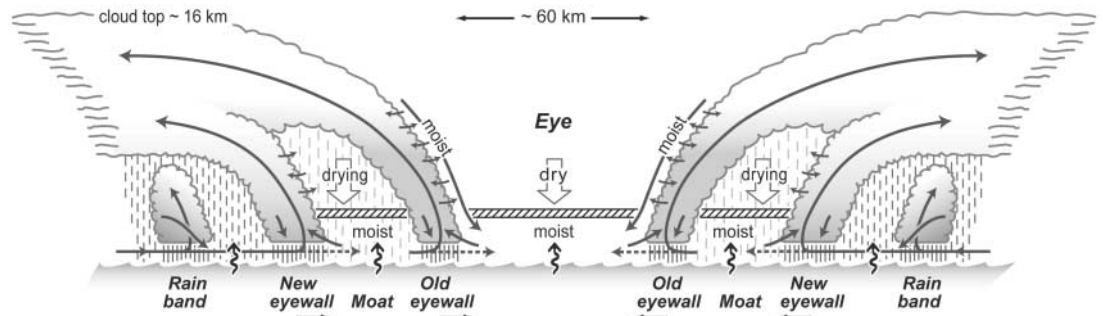


Fig. 3. Relative humidity (A) and temperature (B) profiles measured by dropsondes launched from aircraft in Hurricane Rita. The green curves show data obtained on 21 September (1601 UTC) in the eye of Rita, when the storm was reaching category 5 strength and was still intensifying. It reached its minimum observed pressure of 897 mb about 12 hours later. The red and blue curves show data obtained in Rita 24 hours later, during the eyewall replacement on 22 September 2005, when the central pressure had risen to 915 to 920 mb. The red curves (1619 UTC) show data obtained in the eye. The blue curves (1801 UTC) show the data from one of eight soundings obtained in the moat.

Fig. 4. Inner region of a hurricane undergoing eyewall replacement. The structure of the eye and innermost (original) eyewall are based primarily on (18) and (21). The structure of the rainbands is based on (36). The double-eyewall structure, including the moat separating the two interacting eyewalls, is based on RAINEX observations. Arrows at the bottom indicate



that both eyewalls were contracting inward. The density of vertical lines below the clouds indicates relative precipitation intensity. Thin arrows show the direction of air motion relative to the storm. Dashed segments indicate partially interrupted flow. Small, wavy arrows at the sea surface indicate water vapor mixing upward from the ocean surface. The broad arrows indicate the

downward motion induced by the heating in the eyewall and (possibly) momentum mixing across the inner edges of the eyewalls. The hatched zone shows the top of the near-surface moist layer, which is capped by the stabilizing and drying effect of subsiding air above. The moist layer is not to scale; its depth is exaggerated to show details of the airflow at low levels.

aircraft onto small-scale storm features likely to be associated with storm intensity change could provide timely input that would improve operational forecasts of hurricane intensity.

References and Notes

- This well-known fact is statistically documented at (29).
- R. H. Simpson, J. S. Malkus, *Sci. Am.* **211**, 27 (1964).
- H. E. Willoughby, D. P. Jorgensen, R. A. Black, S. L. Rosenthal, *Bull. Am. Meteorol. Soc.* **66**, 505 (1985).
- R. C. Sheets, in *Hurricane! Coping With Disaster*, R. Simpson, Ed. (American Geophysical Union, Washington, DC, 2003), chap. 3.
- H. E. Willoughby, J. A. Clos, M. G. Shoreibah, *J. Atmos. Sci.* **39**, 395 (1982).
- L. J. Shapiro, H. E. Willoughby, *J. Atmos. Sci.* **39**, 378 (1982).
- R. A. Houze Jr. et al., *Bull. Am. Meteorol. Soc.* **87**, 1503 (2006).
- P. H. Hildebrand et al., *Bull. Am. Meteorol. Soc.* **77**, 213 (1996).
- S. Abernethy et al., *Bull. Am. Meteorol. Soc.* **87**, 1039 (2006).
- M. T. Montgomery, R. J. Kallenbach, Q. J. R. *Meteorol. Soc.* **123**, 435 (1997).
- D. Orrt, S. S. Chen, 27th Conference on Hurricanes and Tropical Meteorology, American Meteorological Society, 24 to 28 April 2006, Monterey, CA, preprint 12A.5 (2006) (available at <http://ams.confex.com/ams/pdffpapers/108643.pdf>).
- Precipitation particles are liquid drops or ice particles heavy enough to be falling relative to Earth's surface. Most meteorological radars, including those deployed on the aircraft in RAINEX, detect precipitation but do not see smaller, non-falling cloud particles. Therefore, the intensity of the radar signal is related to precipitation intensity. The radar also detects the Doppler shift between emitted and received signals, which indicates the speed of movement of the precipitation particles along the beam of the radar. The wind speed and direction can be inferred from the Doppler velocities when the same precipitation particles are observed in more than one radar beam.
- J. P. Kossin, W. H. Schubert, M. T. Montgomery, *J. Atmos. Sci.* **57**, 3890 (2000).
- D. P. Jorgensen, T. Matejka, J. D. DuGranrut, *Meteorol. Atmos. Phys.* **59**, 83 (1996).
- P. D. Reasor, M. T. Montgomery, F. D. Marks Jr., J. F. Gamache, *Mon. Weather Rev.* **128**, 1653 (2000).
- P. Dodge, R. W. Burpee, F. D. Marks Jr., *Mon. Weather Rev.* **127**, 987 (1999).
- E. A. Ritchie et al., in *Hurricane! Coping With Disaster*, R. Simpson, Ed. (American Geophysical Union, Washington, DC, 2003), chap. 12.
- H. E. Willoughby, *Mon. Weather Rev.* **126**, 3053 (1998).
- When air subsides, its relative humidity decreases because the air temperature increases adiabatically. Consequently, saturation vapor pressure rises while the water vapor content remains constant.
- A dropsonde is a package of pressure, temperature, and humidity sensors that is dropped from an aircraft and tracked with a Global Positioning System receiver. The data obtained provide vertical profiles of temperature, humidity, and wind below the aircraft. For further information, see (30).
- K. A. Emanuel, *J. Atmos. Sci.* **54**, 1014 (1997).
- A temperature inversion is not required for a layer of air to be stable, i.e., resistant to vertical mixing. Stability exists in unsaturated air as long as the temperature decrease with height is $>10^{\circ}\text{C}/\text{km}$.
- J. Persing, M. T. Montgomery, *J. Atmos. Sci.* **60**, 2349 (2003).
- M. T. Montgomery, M. M. Bell, S. D. Abernethy, M. L. Black, *Bull. Am. Meteorol. Soc.* **87**, 1335 (2006).
- F. D. Marks Jr., R. A. Houze Jr., *Bull. Am. Meteorol. Soc.* **65**, 569 (1984).
- The hurricane-strength categories 1 to 5 represent, in ascending order, the degree of damage that can be done by the storm. For further details, see (27, 31).
- H. S. Saffir, in *Hurricane! Coping With Disaster*, R. Simpson, Ed. (American Geophysical Union, Washington, DC, 2003), chap. 7.
- The range of the observed winds can be found at (32).
- National Hurricane Center (NHC), www.nhc.noaa.gov/verification.
- Earth Observing Laboratory, National Center for Atmospheric Research, www.eol.ucar.edu/rtf/facilities/dropsonde.
- NHC, www.nhc.noaa.gov/aboutsshs.shtml.
- NHC, www.nhc.noaa.gov/pdf/TCR-AL182005_Rita.pdf.
- Navy Operational Global Atmospheric Prediction System (NOGAPS), www.nrlmry.navy.mil/nogaps_his.htm.
- S. S. Chen, J. F. Price, W. Zhao, M. A. Donelan, E. J. Walsh, *Bull. Am. Meteorol. Soc.*, in press; available at http://orca.rsmas.miami.edu/~schen/publications/Chenetal_InBox_CBLAST_final_8Sept06.pdf.
- In RAINEX, the high-resolution MMS was run with input from four different global models. The input from NOGAPS (33) gave the best result for Hurricane Rita. Also see (7).
- G. M. Barnes, E. J. Zipser, D. Jorgensen, F. D. Marks Jr., *J. Atmos. Sci.* **40**, 2125 (1983).
- Aircraft operations in RAINEX were under the direction of C. Newman (NRL aircraft) and J. MacFadden (NOAA aircraft). Lead airborne missions scientists for RAINEX included R. Rogers, M. Black (NOAA Hurricane Research Division), and D. Jorgensen (NOAA National Severe Storms Laboratory). Daily aircraft mission planning was led by J. Moore and G. Stossmeister (University Corporation for Atmospheric Research), and D. Nolan (University of Miami) contributed scientific guidance to the planning. Engineering support for ground control of flights was provided by C. Burghart and J. Scannel (NCAR), P. Chang (NOAA National Environmental Satellite, Data, and Information Service), J. Carswell (Remote Sensing Solutions, Inc.), and S. Brodzik (University of Washington). Engineering support for the radar and dropsonde measurements was directed by E. Loew, M. Strong, H.-Q. Cai, and E. Korn (NCAR). Real-time high-resolution model runs were carried out by W. Zhao (University of Miami). Forecasting for flight operations was done by J. Cangialosi and D. Orrt (University of Miami). G. Stossmeister and J. Meitin (University Corporation for Atmospheric Research) provided web support and data management for the project. B. Tully (University of Washington) coordinated the graphics. This research was supported by NSF grants ATM-0432623 and ATM-0432717.

27 September 2006; accepted 19 January 2007
10.1126/science.1135650

Chankillo: A 2300-Year-Old Solar Observatory in Coastal Peru

Ivan Ghezzi^{1,2,3*} and Clive Ruggles⁴

The Thirteen Towers of Chankillo run north to south along a low ridge within a fourth-century B.C.E. ceremonial complex in north coastal Peru. From evident observing points within the adjacent buildings to the west and east, they formed an artificial toothed horizon that spanned—almost exactly—the annual rising and setting arcs of the Sun. The Chankillo towers thus provide evidence of early solar horizon observations and of the existence of sophisticated Sun cults, preceding the Sun pillars of Incaic Cusco by almost two millennia.

The identification of places from which astronomical observations were made in prehistory, together with evidence on the nature and context of those observations, can reveal much about the ways in which people before the advent of written records perceived, understood, and attempted to order and control the

world they inhabited (1, 2). Evidence of systematic observations of the changing position of the rising and setting Sun along the horizon (3), in particular, can provide information on the development, nature, and social operation of ancient calendars (4). Solar horizon calendars were certainly important among indigenous Americans, with one of the best-known modern examples being at the Hopi village of Walpi (5). In Mesoamerica before European contact, systematic studies of the orientations of sacred buildings and city plans strongly suggest the existence of horizon calendars in which special meaning was attributed to certain key dates. It has been argued that these dates included not only the solstices but

also the dates of solar zenith passage (6) and dates counted off from both at intervals that were important in the intermeshing cycles of the Mesoamerican calendar round (7). In South America, accounts going back to the 16th century C.E. record various details of indigenous practices relating to Inca state-regulated Sun worship and related cosmological beliefs (8, 9). Various schemes of landscape timekeeping have been suggested, which are supported by a combination of historical evidence and analyses of the spatial disposition of sacred architecture: in particular, the system of shrines placed along lines (*ceques*) conceived as radiating out from the central Sun temple, the Coricancha, in Cusco, Peru (10–12). “Sun pillars” are described by various chroniclers as having stood around the horizon from Cusco and been used to mark planting times and regulate seasonal observances (13), but all the Cusco pillars have vanished without trace and their precise location remains unknown. Here, we describe a much earlier structure in coastal Peru that seems to have been built to facilitate sunrise and sunset observations throughout the seasonal year.

The group of structures known as the Thirteen Towers is found within Chankillo, a ceremonial center in the Casma-Sechín River Basin of the coastal Peruvian desert (fig. S1). Seventeen ¹⁴C dates fall between 2350 and 2000 calibrated years

¹Instituto Nacional de Cultura, Avenida Javier Prado Este 2465, Lima 41, Peru. ²Pontificia Universidad Católica del Perú, Avenida Universitaria Cuadra 18, Lima 32, Peru. ³Yale University, 51 Hillhouse Avenue, New Haven, CT 06511, USA. ⁴School of Archaeology and Ancient History, University of Leicester, Leicester LE1 7RH, UK.

*To whom correspondence should be addressed. E-mail: ighezzi@yahoo.com